Dynamic response of single crystalline copper subjected to quasi-isentropic laser and gas-gun driven loading

M. Meyers[1], H. Jarmakani[1], J.M. McNaney[2], M. Schneider[1], J.H. Nguyen[2] and B. Kad[1]

[1] *Mechanical and Aerospace Engineering Dept., Materials Science Program, University of California, San Diego, La Jolla, CA 92093-0418, USA*
[2] *Lawrence Livermore National Laboratory, Livermore, CA 94550, USA*

Abstract. Single crystalline copper was subjected to quasi-isentropic compression via gas-gun and laser loading at pressures between 18 GPa and 59 GPa. The deformation substructure was analyzed via transmission electron microscopy (TEM). Twins and laths were evident at the highest pressures, and stacking faults and dislocation cells in the intermediate and lowest pressures, respectively. The Preston-Tonks-Wallace (PTW) constitutive description was used to model the slip-twinning process in both cases.

1. INTRODUCTION

The consituitive response of a material to dynamic loading depends on the deformation mechanisms that are activated. These mechanisms are, in turn, dependent on the properties of the material and the test conditions. The response of copper to very high strain-rate deformation is reasonably well understood. Copper is known to display both classical slip-based deformation, wherein strain accommodation is accomplished through dislocation multiplication and motion, and twinning, which occurs at relatively higher pressures [1]. The residual signatures of these two mechanisms are distinctly different and easily discernable via methods like transmission electron microscopy (TEM). Different FCC metals have different threshold twinning pressures depending upon their stacking-fault energies. This current work aims to understand the dynamic response of [001] oriented single crystalline copper under quasi-isentropic loading and shed light on the competing slip-twinning transition under such loading. An isentropic compression experiment (ICE) is a shockless process whereby the pressure rise is gradual, smooth and controlled, and the accompanying temperature rise is much less severe, as compared to shock loading. The main motivation behind such a process is that the solid state of a material subjected to extreme pressures can be retained due to the lower temperatures experienced during ICE, and an understanding and characterization of the material response is, therefore, possible. The quasi-isentropic compression conditions in this work are achieved via two different methods: gas-gun and laser loading. Experiments having the closest peak pressures in both cases are reported for a comparative study.

2. EXPERIMENTAL PROCEDURE

2.1 ICE experimental setup: Gas-gun

A two-stage gas-gun set-up located at LLNL provided for the quasi-isentropic loading. It employs functionally-graded material (FGM) impactors designed with increasing density profiles (or shock impedance), as depicted in Fig. 1(a), to produce the smoothly rising pressure profiles. Three different FGMs were used, each providing a certain density range. A detailed description of the impactors can be found in [2]. Three experiments, **A** (52 GPa, 1700 m/s), **B** (26 GPa, 1260 m/s) and **C** (18 GPa, 730 m/s) are reported. The as-received samples belonging to each batch were in the form of cylindrical specimens having an average diameter and thickness of 6 mm and 3.6 mm, respectively. Two distinct
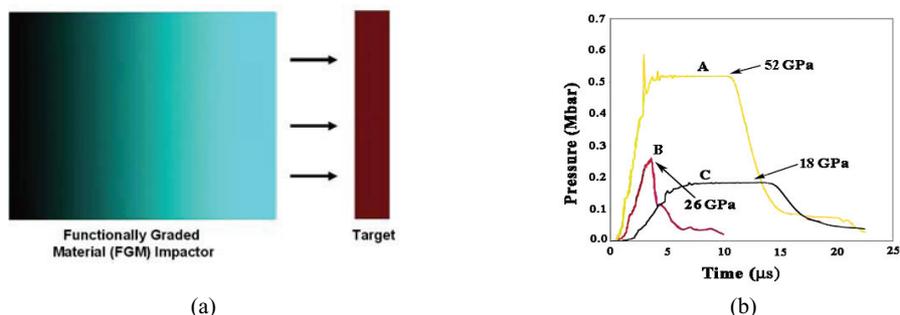
Figure 1. (a) Illustration of FGM impactor hitting a target (darkness proportional to density); (b) Pressure vs. time profile of gas-gun experiments.

pressure profiles were obtained using CALE, a hydrodynamics simulation code [3]; one having a hold-time of approximately 10 μs (**A** and **C**) and one having relatively no hold time (**B**), as shown in Fig. 1(b). It should be noted that **A** exhibited a spike or slight shock at the onset of the pulse duration due to the experimental setup and the likely effect on the microstructural deformation process is briefly discussed in the results section. Strain rates obtained via CALE were on the order of 10^4 s^{-1}, 10^5 s^{-1} lower than laser driven ICE.

2.2 ICE experimental set-up: laser

The Omega Laser System at the University of Rochester, NY, was used to generate a smoothly rising pressure pulse in the material. This pulse is created by focusing a laser beam on a reservoir material (carbon foam) facing the sample and separated from it by a necessary vacuum gap ($\sim$ 250 μm). The beam creates a plasma that "stretches out" through the vacuum and discharges onto the sample. The strain-rates achieved with this set up were on the order of 10^7 s^{-1}, three orders of magnitude higher than that of the gas-gun experiments. McNaney et al. [4] use the same shockless laser drive setup to compress and recover [001] copper and a more detailed description of the setup can be found in their publication. An illustration of the setup is provided in Fig 2(a) accompanied by a typical pressure profile modeled by CALE, Fig. 2(b) [4]. The three peak pressures reported for the laser ICE experiments are 18 GPa, 24 GPa, and $\sim$59 GPa, very reasonably close to the gas-gun pressures. The pressure estimate of 59 GPa is more uncertain than the others because of the lack of benchmarking the data for the reservoir used in the experiment. An extrapolation from higher pressure data was done instead.
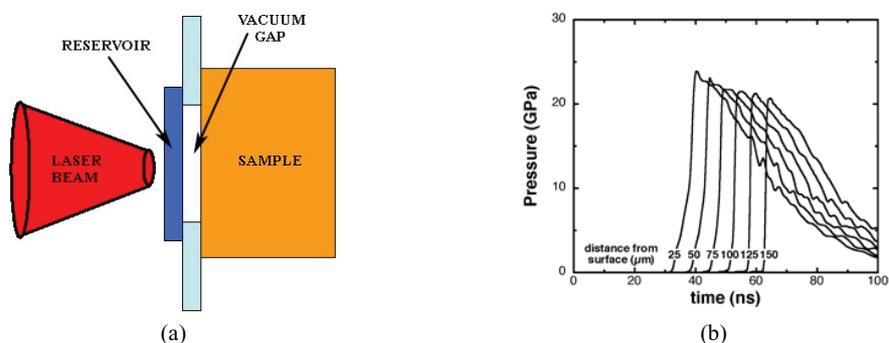
Figure 2. a) Schematic of the laser ICE setup; b) Typical pressure vs. time profile obtained, ($\sim$24 GPa).

2.3 TEM sample preparation

For the gas-gun samples, 3 mm diameter cylinders were cut out from the impacted samples by electro-discharge machining (EDM). Four TEM foils were then sliced from each cylinder and further polished down to approximately 100 μm. The foils were electropolished using a solution of 7% H_2SO_4 in methanol. In the case of the laser ICE samples, more care had to be given to sample preparation since quasi-isentropic loading was only limited to the area near the bottom of the crater ($\sim$120 μm). The near isentropic wave eventually steepens into a shockwave as it traverses the material, and both regimes have very different operative deformation mechanisms. Discs having a diameter of 3 mm were cut through the center of the impacted sample and further mechanically ground to approximately 100 μm with extreme care such that the deepest part of the crater was not polished away. A 30% nitric acid in methanol solution was used for electropolishing. A dummy copper sample was used to cover the front end (cratered surface) of the loaded specimen for the initial polishing which lasted 45 seconds and corresponded to 50 μm of material being polished away from the back surface. The dummy specimen was then removed and a final polishing occurred such that the hole formed at a distance less than 25 μm from the loaded surface. All samples were sent to Oak Ridge National Labs, where TEM was performed, under the SHaRE program, to characterize the operative deformation mechanisms. Efforts were made to examine and document all visible regions of the samples as it was observed that the operative mechanisms could differ from region to region.

3. RESULTS AND DISCUSSION

3.1 TEM: Gas-gun ICE

TEM samples analyzed from **A** (52 GPa) revealed various deformation substructures. Dislocation activity was most abundant, however, other deformation features were found. At approximately 0.1 mm from the impact surface, some limited evidence of twining was found. Fig. 3(a) shows very clear twinned regions. At a beam direction of B = [011], both small and large twins were observed having ($\bar{1}\bar{1}1$) twin habit planes. These micro-twins are embedded within dislocated laths running along the same direction. The smallest twins measured had lengths of approximately 80 nm, and the longest twins were on the order of 1.5 μm. TEM images (not shown here) taken at the same depth with B=[001] showed twins running along the [$\bar{2}$20] and [220] at 90° from each other. In certain areas of the sample, single lath variants and stacking faults with thicker features running long the [$\bar{2}$20] and [$\bar{2}\bar{2}$0] directions were captured. It is suggested that these substructures are due to thermal recovery. At 0.7 mm and 1.2 mm from the surface, heavily dislocated laths running along the [220] direction were observed having an average thickness of 0.6 μm and 0.7 μm, respectively. Twinning, confirmed by a diffraction pattern was
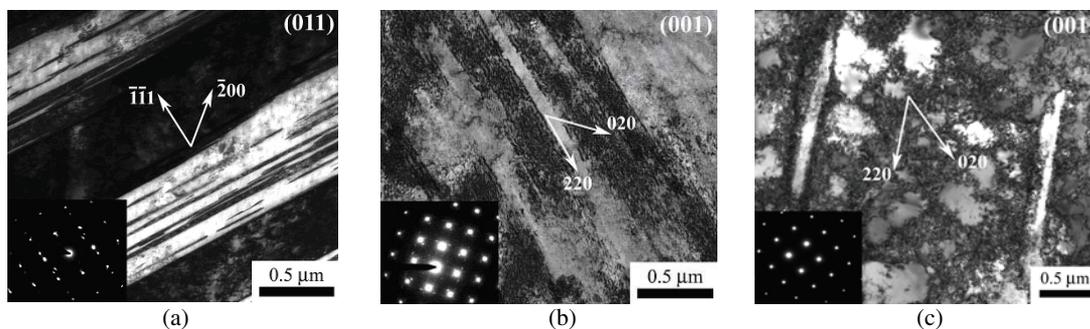
Figure 3. (a) Twinned regions $\sim$0.1mm from surface, 52 GPa.; (b) Stacking faults at 1.3 mm running along [220], 26 GPa; (c) Elongated and regular cells at 0.13 mm, 18 GPa.

evident at 1.2 mm. The average dislocation cell size at this depth was 0.15 μm. At 1.8 mm, dislocation cells with an average size of 0.2 μm were mostly abundant.

Foils from **B**, (26 GPa), mostly revealed dislocation cells, where the average cell size increased from 0.4 μm at 0.25 mm within the sample to 0.5 μm at 2.7 mm. At 0.9 mm and 1.3 mm from the impact surface, stacking faults were evident in a few isolated regions running along the [220] orientation, Fig. 3(b). Dislocated laths at 1.8 mm and elongated dislocation cells at 2.3 mm away from the impacted surface were observed stretched along the [220] direction. For experiment **C** (18 GPa), relatively large dislocation cells were the most abundant deformation substructure, Fig. 3(c). The average dislocation cell size varied from approximately 0.5 μm at 0.13 mm within the specimen to 0.6 μm at 2 mm. Elongated cells along the [220] direction were observed and some lath-like features were noticed in some regions, in particular closest to the impact surface at $\sim$0.1 mm within the sample. The elongated cells seem to have relaxed from the dislocated lath structures located at regions experiencing higher pressures closer to the impact surface.

3.2 TEM: Laser ICE

At the highest pressure of approximately 59 GPa, a large number of faults/twins was observed, Fig. 4(a). They were preferentially oriented along the [022], identical to what has been reported in laser shocked copper [5] and the gas-gun ICE experiments. They were found near regions of extremely high dislocation densities. Laths spaced at regular intervals of 500 nm (also their average width) were also observed with heavily dislocated regions in between. At a lower pressure of 24 GPa, stacking faults were dominant. An interesting image, Fig. 4(b), was taken of a transitional substructure showing dislocation cells to the right and stacking faults to the left. The average dislocation cell size was 0.2 μm and the cells were comprised of $\langle 110 \rangle$ type dislocations. The stacking faults were identical to the four variants observed in laser shock compression having a $\{111\}1/6\langle 112 \rangle$ nature. The average spacing was 650 nm with a width of nearly 150 nm. There was no visible difference in the material that contained cells and the area that contained stacking faults. The imaged area was taken from near the center of the sample and deepest part of the crater.

Dislocation cells, Fig. 4(c), similar to those observed in shock loading were the predominant mode of deformation for the samples loaded to 18 GPa. The defects were primarily $1/2 \langle 110 \rangle$ type dislocations which have relaxed into cells. The cell sizes measured in the isentropic specimens at this pressure were approximately 0.3 μm,. It is interesting to note that one unique characteristic of the isentropic compression was the uniformity of the cell sizes at the given pressure. Unlike shock loading where there was substantial variance between cell sizes [5], the quasi-isentropically loaded specimens were very similar in size and shape. Also, the dislocation cells were more clearly defined as compared to laser shocked samples previously studied [5]. This is likely a result of the isentropic loading conditions.

(a)   (b)   (c)
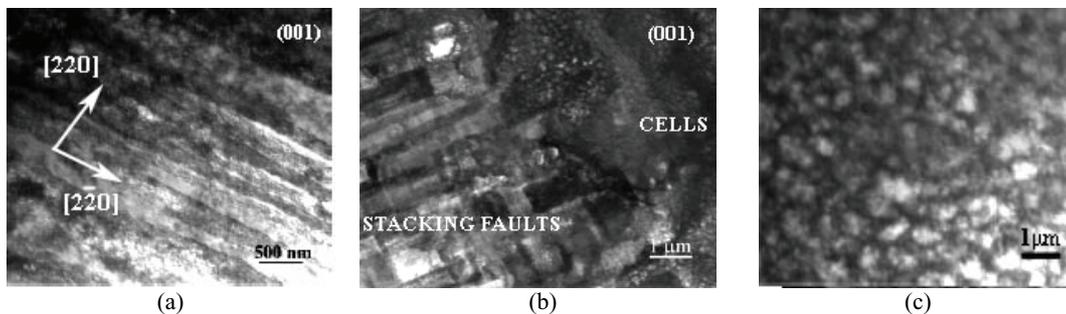
Figure 4. (a) Twins/laths at 59 GPa; (b) Dislocation cells and stacking faults at 24 GPa; (c) Dislocation cells at 18 GPa.

3.3 Twinning threshold modeling

The Prenston-Tonks-Wallace (PTW) [6] constitutive description is used to determine the critical pressure for twinning in both laser and gas-gun quasi-isentropic compression, as it is very suitable for the very high strain-rates in these experiments. It takes into account both the thermal activation and dislocation drag regimes. The instantaneous flow stress can be calculated from:

$$\tau = \hat{\tau}_s + \frac{1}{p}(s_0 - \hat{\tau}_y)\ln\left\{1 - \left[1 - \exp\left(-p\frac{\hat{\tau}_s - \hat{\tau}_y}{s_0 - \hat{\tau}_y}\right)\right]\exp\left[\frac{-p\theta\psi}{(s_0 - \hat{\tau}_y)\left[\exp\left(p\frac{\hat{\tau}_s - \hat{\tau}_y}{s_0 - \hat{\tau}_y}\right) - 1\right]}\right]\right\} \quad (1)$$

where $\hat{\tau}_s$ and $\hat{\tau}_y$ are the work hardening saturation stress and yield stress, respectively. Separate expressions modeling $\hat{\tau}_s$ and $\hat{\tau}_y$ in both the thermal activation regime and strong shock regime are provided by PTW (not given here for conciseness). s_0 is the value of $\hat{\tau}_s$ taken at zero temperature, ψ and θ are the strain and work hardening rate, respectively, and p is a dimensionless material parameter. The flow stress is normalized to the shear modulus, G. e.g., $\hat{\tau}_y = \tau_y/G$. Where appropriate the temperature dependence of the shear modulus was approximated as $G(\rho, T) = G_0(\rho)(1 - \alpha\hat{T})$, where $G_0(\rho)$ is the zero temperature modulus as a function of density and α is a material constant. The pressure dependence of the model is due to the pressure dependence of the shear modulus.

The model parameters were slightly modified to match the low strain rate work hardening behavior for $\langle 100 \rangle$ copper. In particular the work hardening rate, θ, was adjusted to a value of 0.01 and saturation stress, s_0, to a value of 0.0045. All other parameters are as given in [6]. In the shocked region, the temperature and strain were taken from the simulations while the strain rates were determined from the Swegle-Grady relation [7]. It has also been assumed that the flow stress and twinning stress, being dependent on the atomic energy barrier, scale with the shear modulus, as is typical in high pressure constitutive models. Results of these calculations are presented in Fig. 5, where the flow stress, as a function of peak drive pressure, for the shockless and shocked region are plotted for both quasi isentropic gas-gun and laser compression. The twinning threshold was assumed to vary with pressure through the density dependence of G:

$$\sigma_T(P) = \sigma_T^0 \frac{G(T, P)}{G_0} \quad (2)$$
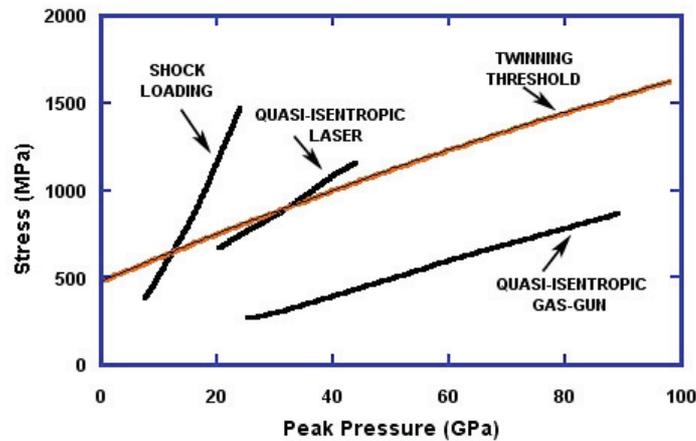
Figure 5. Flow stress vs. peak pressure for shock compression, gas-gun ICE and laser ICE.

where σ_T^0 and G_0 are the twinning threshold stress and shear modulus at ambient pressure respectively. It can be seen that a slip-twinning transition does not occur during gas-gun loading, and a twinning threshold stress should, therefore, not be reached. This is inconsistent with experimental observations at 52 GPa, since twinning was observed at that pressure. The presence of the shock at the start of the shock pulse (Fig. 1(b)) for this pressure condition creates a deviation from quasi-isentropic conditions and may be accountable for the presence of the twins observed. In the case of laser ICE, the threshold lies at 32 GPa, consistent with observations of the lack of twinning at 24 GPa and 18 GPa, and their presence at $\sim$59 GPa. The steep shock loading curves in both cases arise due to the high strain-rate dependence on both the shock pressure and flow stress [7].

4. CONCLUSIONS

In this study, [001] mono-crystalline copper is quasi-isentropically compressed via gas-gun and laser from 18 GPa to $\sim$59 GPa. The microstructure is characterized via TEM with emphasis on the slip to twinning transition. Gas-gun experiments revealed twinning closest to the impact surface at 52 GPa. Dislocated laths, stacking faults and dislocation cells were revealed in the intermediate pressure regime of 26 GPa, and dislocation cells were mostly abundant at the lowest pressure of 18 GPa. Dislocation activity decreased with increasing distance from the impact surface for all experiments. The laser ICE experiments revealed dislocated laths due to thermal recovery as well as twins at the highest pressure of 59 GPa. At a lower pressure of 24 GPa, stacking faults were abundant, and at 18 GPa, relatively smaller uniform dislocation cells were evident. The Preston-Tonks-Wallace description was used to model the twinning threshold in both cases, and a reasonable agreement with experiments was established.

References

[1] Johari, O. and Thomas, G., "Substructures in Explosively Deformed Cu and Cu-Al alloys. Acta Metall., 2:113-1159 (1964).
[2] Nguyen, J. H., Orlikowski, D., Streitz, F. H., Holmes, N. C., and Moriarty, J. A., "Specifically Prescribed Dynamic Thermodynamic Paths and Resolidification Experiments, Shock Compression of Condensed Matter, M. D. Furnish, L.C. Chhabildas, and R. S. Hixson, Eds., AIP Conf. Proc., Melville, New York (2004).
[3] Tipton, R., Managan, R., and Amala, P., CALE Users Manual, 2002, Lawrence Livermore National Laboratory.
[4] McNaney et al., High Pressure, "High Strain-Rate Behavior in Single Crystal Copper Using Laser Based Loading Platform:Shockless to Shocked Transition"., In Press, Acta Mat (2006).
[5] Schneider, M. S., Kad, B. K., Kalantar, D. H., Remington, B. A., and Meyers, M. A., "Laser-Induced Shock Compression of Copper: Orientation and Pressure Decay Effects." Met Trans A, 35 A, 263 (2004).
[6] Preston, D. L., Tonks, D. L., and Wallace, D. C., "Model for Plastic Deformation for Extreme Loading Conditions", J. Applied Physics, 93, 211 (2003).
[7] Swegle, J. W., and Grady, D. E., J. Applied Physics, 58, 692 (1985).